Momentum-dependent *s*-wave and *d*-wave interactions in atomic Bose-Einstein condensates

Moumita Gupta[1,*] and Krishna Rai Dastidar[2,†]
[1]*Kamala Girls' School, P-512, Lake Road Extn., Kolkata 700029, India*
[2]*Indian Association for the Cultivation of Science, Kolkata 700032, India*
and LAMP Group, Raman Research Institute, Bangalore-560080, India

(Received 23 January 2013; revised manuscript received 20 August 2013; published 17 September 2013)

We investigate the role of momentum-dependent interactions to determine the ground-state properties in the Bose-Einstein condensate for large scattering lengths (a) such that $ka \geqslant 1$, even for small momentum (p) where $p = \hbar k$ and k is the wave number. The results for momentum-dependent and momentum-independent interactions differ significantly, even for moderate values of a, and the effect of higher partial-wave interaction increases with the increase in a. We have made an attempt to compare the theoretical column density with experimental results at different magnetic fields [Cornish *et al.*, Phys. Rev. Lett. **85**, 1795 (2000)]. Since the initial number of atoms changes while swapping the magnetic field and the actual value of the number of atoms at different magnetic fields is not known, we studied the dependence of column densities on the value of N at different magnetic fields. We present here the results for those values of N for which the theoretical column densities are comparable with the experimental results. It is shown that the column density for ^{85}Rb atoms at 100 nK with momentum-dependent interaction is in fairly good agreement with the experimental values for different values of N at two different values of magnetic fields ($B = 157.2$ and 156.4 G).

DOI: 10.1103/PhysRevA.88.033619 PACS number(s): 03.75.Hh, 03.75.Kk

I. INTRODUCTION

For a very dilute Bose-Einstein condensate (BEC), which is the case in most of the experiments, the interatomic interaction is sufficiently weak and the mean-field Gross-Pitaevskii theory is a logical tool to study such a system [1]. The physics of cold atom scattering is dominated by the two-body contact interaction, which is well described by the s-wave scattering length. In this case the momentum dependence of interatomic interaction is neglected, since $ka \ll 1$, where k is the wave number (momentum $p = \hbar k$) and a is the scattering length of the atoms. In BECs the momentum of the interacting atoms is small, and if the scattering length is confined to a moderate value ($\ll$1000 a_0 for 100-nK temperature), the momentum dependence of the interaction can be neglected [2,3]. It is well known that the interatomic interaction can be tuned to different values by varying the scattering length and in this process ka may exceed unity, although the momentum is small for such systems. Hence when $ka \geqslant 1$, the momentum dependence of the interatomic interaction cannot be neglected. Recent experiments [4–6] have explored the possibilities of increasing the scattering length by exploiting the magnetic Feshbach resonance. In the experiment performed at JILA [4], the scattering length of the ^{85}Rb (cylindrically trapped 10^4 atoms at 100 nK) was varied from negative value to 10,000 a_0 by swapping the magnetic field through Feshbach resonance ($B \approx$ 155 G). In this case ka becomes greater than unity at and above $a = 3000\, a_0$, and hence the momentum-dependent interaction becomes important. The ^{85}Rb system has been used in several experiments to explore the physics of interacting quantum systems [4,7,8]. Properties of cold Bose gases in the regime of large scattering length has been studied [9,10]. Calculation of the interspecies scattering length for the sodium-rubidium (Na-Rb) system has also been reported [11].

The first-order theory of Beliaev [2] gives the momentum dependence of scattering amplitude by applying field-theoretic diagrammatic treatment to the zero-temperature homogeneous dilute interacting Bose gas [2,12]. Subsequently, Beliaev's theory was generalized to give the temperature dependence of the excitation spectrum of Bose gas [13,14]. In the regime $ka \ll 1$, Beliaev's first-order theory reduces to the Bogoliubov spectrum [15] for contact potential. The work of Lee, Huang, and Yang (LHY) [16,17] on the low-temperature properties of dilute hard sphere gas considering the perturbation theory gives the first correction to the Bogoliubov mean-field theory for dilute gases for relatively stronger interaction. The energy correction obtained from Beliaev's second-order theory [2] coincides with the LHY correction. Brueckner and Sawada also determined the quantum depletion and correction to the ground-state energy of a homogeneous dilute Bose gas [18]. To study the ground-state and dynamic properties of a dilute Bose gas with strong interactions, momentum-dependent scattering of atoms along with the contribution from LHY correction needs to be considered.

Our aim here is to emphasize the significance of the momentum (k)-dependent scattering amplitudes (both for s-wave and higher partial-wave scattering) to determine the ground-state properties and the column densities of the system for large scattering lengths ($ka > 1$) even at small values of momentum. For strongly interacting systems ($ka \gg 1$), the higher-order partial waves are likely to give significant contribution to the scattering amplitudes. For Bose gases only the even partial waves will contribute. It has been mentioned by Beliaev [2] that the d-wave contribution to the energy spectrum can be $\sim$10%. Here we will show that d-wave contribution to the column density can be more significant at the center of the trap for large values of scattering length.

In this paper we present the ground-state energy functional of trapped atomic Bose-Einstein condensate, including the effect of momentum-dependent scattering and also including the LHY correction term. Higher partial-wave interactions

*E-mail: mou_mita_81@yahoo.co.in
†E-mail: krishna_raidastidar@yahoo.co.in

have been incorporated in the energy functional. From the ground-state energy functional the time-independent equation has been derived to give the condensate density. We have considered cylindrically trapped 10^4 ^{85}Rb atoms at 100 nK with the scattering length varying from 3000 a_0 to 8700 a_0. The corresponding range of variation of ka is 1.15–3.33, and the values of the peak gas parameter $x_{pk} \sim 10^{-2}$ [$x_{pk} = n(0)a^3$, where $n(0)$ is the peak density of Bose gas]. Column densities considering k-independent scattering have been compared with those for k-dependent s- and $(s+d)$-wave scattering (including the LHY correction term) in a situation where (i) the number of atoms has been kept fixed and the scattering length is varied or (ii) the scattering length is kept fixed and the number of atoms is allowed to vary in a range of values. The results obtained by solving Gross-Pitaevskii (GP) equation (i.e., without including LHY interaction) have also been given for comparison. It is found that for $ka > 1$, the contribution of the momentum-dependent scattering (s-wave and higher partial waves) to the column density becomes important and the nature of column density differs significantly from that obtained for k-independent scattering (contact interaction with LHY correction). As in the vicinity of Feshbach resonance the two- and three-body loss rates play a crucial role [19–22], their effects have also been included phenomenologically in the time-independent equations of the condensate. The patterns of the column densities as observed experimentally agree fairly well with our results, considering momentum-dependent interactions at $B = 157.2$ G ($a \approx 3000\ a_0$) and $B = 156.4$ G ($a \approx 8700\ a_0$). However, the long tail part of the density profile away from the center of the trap could not be explained.

II. THEORY

Using partial-wave expansion, the scattering amplitude for identical bosons can be expressed as

$$f(\theta) = (1/k)\sum_{l=0}^{\infty}(2l+1)\exp(i\delta_l)\sin\delta_l P_l(\cos\theta), \qquad (1)$$

where l denotes partial waves, δ_l is the phase shift, and θ is the scattering angle [23]. For identical bosons only even values of l will contribute to the scattering amplitude. According to Beliaev's first-order theory, the excitation spectrum of a dilute Bose gas can be given by the dispersion relation

$$\epsilon_k^{(1)} = \sqrt{\left[\epsilon_k^0 + 2n_0 f^s\left(\frac{k}{2},\frac{k}{2}\right)\frac{\hbar^2}{m} - n_0 f(0,0)\frac{\hbar^2}{m}\right]^2 - \left[n_0 f(k,0)\frac{\hbar^2}{m}\right]^2}, \qquad (2)$$

where $\epsilon_k^0 = \hbar^2k^2/(2m)$ is the kinetic energy and m is the atomic mass. The two distinct scattering amplitudes (considering s-wave) are

$$f(0,0) = 4\pi a$$

and

$$f(k,0) = 4\pi\,\sin(ka)/k. \qquad (3)$$

The symmetrized amplitude $f^d(k/2,k/2)$ for the higher partial wave ($l = 2$) is added with $f^s(k/2,k/2)$ (for $l = 0$) to give the following dispersion relation:

$$\epsilon_k^{(1)} = \sqrt{\left\{\epsilon_k^0 + 2n_0\left[f^s\left(\frac{k}{2},\frac{k}{2}\right) + f^d\left(\frac{k}{2},\frac{k}{2}\right)\right]\frac{\hbar^2}{m} - n_0 f(0,0)\frac{\hbar^2}{m}\right\}^2 - \left(n_0 f(k,0)\frac{\hbar^2}{m}\right)^2}. \qquad (4)$$

The values of symmetrized scattering amplitudes considering s and d waves are

$$f^s(k/2,k/2) = 4\pi[\sin(ka) - i2\sin^2(ka/2)]/k$$

and

$$f^d(k/2,k/2) = -40\pi(\cos\delta_2\sin\delta_2 + i\sin^2\delta_2)/k,$$

where

$$\delta_2 = \tan^{-1}\left\{\left[3\frac{ka}{2}\cos\frac{ka}{2} - \left(3 - \frac{k^2a^2}{4}\right)\sin\frac{ka}{2}\right]\right\} \Big/ \left\{\left[\left(3 - \frac{k^2a^2}{4}\right)\cos\frac{ka}{2} + 3\frac{ka}{2}\sin\frac{ka}{2}\right]\right\}.$$

To derive d-wave scattering amplitude only the forward scattering of atoms is considered.

The LHY correction term for the ground-state energy of a dilute Bose gas is

$$E[n] = (2\pi\hbar^2 an)128(na^3/\pi)^{1/2}/(15m). \qquad (5)$$

From the ground-state energy functional, by performing a functional variation with respect to ψ^* the Euler-Lagrange equation [24,25] takes the following form:

$$\left(-\frac{\hbar^2}{2m}\nabla^2 + V_{tr} + g_1|\psi|^2 + \frac{3}{4}\frac{g_1^2 - g_2^2}{\epsilon_k^0}|\psi|^4 + \frac{128}{3}\frac{\hbar^2}{m}\sqrt{\pi}a^{5/2}|\psi|^3\right)\psi = \mu\psi, \qquad (6)$$

where μ is the chemical potential which accounts for the conservation of number of particles, where

$$g_1 = \frac{\hbar^2}{m}\{2[f^s(k/2,k/2) + f^d(k/2,k/2)] - f(0,0)\}$$

and

$$g_2 = \frac{\hbar^2}{m} f(k,0). \tag{7}$$

The trapping potential $V_{tr}(\mathbf{r})$ is taken to be axially symmetric,

$$V_{tr}(\mathbf{r}) = \tfrac{1}{2}m\left(\omega_\perp^2 r_\perp^2 + \omega_z^2 z^2\right), \tag{8}$$

where $\omega_\perp$ and ω_z are the radial and axial frequencies of the cylindrical trap. In g_1 and g_2 the imaginary part of the scattering amplitudes has not been taken into account, as in the first-order Beliaev's theory it is sufficient to take the real part of the scattering amplitude when using it to calculate the spectrum [3].

In Eq. (6) the two-body dipolar (K_2) and three-body recombination (K_3) loss rates are introduced phenomenologically to give

$$\left[-\frac{\hbar^2}{2m}\nabla^2 + V_{tr} + g_1|\psi|^2 + \frac{3}{4}\frac{g_1^2 - g_2^2}{\epsilon_k^0}|\psi|^4 + \frac{128}{3}\frac{\hbar^2}{m}\sqrt{\pi}a^{5/2}|\psi|^3 - \frac{i\hbar}{2}(K_2|\psi|^2 + K_3|\psi|^4)\right]\psi = \mu\psi. \tag{9}$$

At small momenta ($ka < 1$), neglecting the d-wave scattering and setting $f^s(\frac{k}{2},\frac{k}{2}) = f(k,0) = f(0,0)$, Eq. (6) reduces to

$$\left[-\frac{\hbar^2}{2m}\nabla^2 + V_{tr} + g_1'|\psi|^2 + \frac{128}{3}\frac{\hbar^2}{m}\sqrt{\pi}a^{5/2}|\psi|^3\right]\psi = \mu\psi, \tag{10}$$

where $g_1' = 4\pi\hbar^2 a/m$. Equation (10) is known as modified Gross-Pitaevskii (MGP) equation for the atomic condensate [26]. By neglecting the LHY term from the MGP Eq. (10), one gets the corresponding Gross-Pitaevskii (GP) equation as given below:

$$\left[-\frac{\hbar^2}{2m}\nabla^2 + V_{tr} + g_1'|\psi|^2\right]\psi = \mu\psi. \tag{11}$$

The column density, which is an accessible experimental quantity, is defined as $n_c(z) = \int dr_\perp |\psi(r_\perp,z)|^2$. A measure of the extension of the condensate is the half-width of the column density $R_{1/2}$, defined as the z value when $n_c(z = R_{1/2}) = \frac{1}{2}n_c(z = 0)$.

III. RESULTS AND DISCUSSION

In this section we first report the results for ground-state properties and column densities for ^{85}Rb BEC considering k-independent and k-dependent interactions confined in a cylindrical trap. The radial (axial) frequency of the trap is $\omega_\perp/2\pi = 17.5$ Hz ($\omega_z/2\pi = 6.8$ Hz). We have considered here the large gas parameter values ($\sim 10^{-2}$) as achieved in the experiment of Cornish *et al.* [4]. We have compared the theoretical density profiles (both for k-dependent and k-independent interactions) with the experimental results at $a = 3000\ a_0$ and $8700\ a_0$.

TABLE I. Results for the ground-state properties of 10^4 ^{85}Rb atoms trapped in a cylindrically symmetric trap with $\frac{\omega_\perp}{2\pi} = 17.5$ Hz and $\frac{\omega_z}{2\pi} = 6.8$ Hz. Chemical potentials are in the units of $\hbar\omega_\perp$; half-widths are in the units of μm. Results are given for k-dependent s-wave scattering [$s(k)$], k-dependent $(s+d)$-wave scattering [$(s+d)(k)$], and k-independent s-wave scattering [s], including the LHY term. The GP results are also tabulated.

a (a_0)	ka		μ	x_{pk}	Half-width
3000	1.15	$s(k)$	12.47	3.89(–3)	21.01
		$(s+d)(k)$	12.59	3.84(–3)	21.09
		s	14.48	3.19(–3)	22.42
		GP	13.23	3.91(–3)	20.86
5000	1.92	$s(k)$	12.74	1.49(–2)	22.52
		$(s+d)(k)$	13.79	1.37(–2)	23.09
		s	18.77	9.72(–3)	25.88
		GP	16.25	1.33(–2)	23.14
7000	2.68	$s(k)$	11.51	3.61(–2)	23.72
		$(s+d)(k)$	15.15	2.97(-2)	25.15
		s	22.56	1.96(–2)	28.62
		GP	18.61	2.98(–2)	24.76
8700	3.33	$s(k)$	11.16	5.89(–2)	25.15
		$(s+d)(k)$	17.79	4.45(–2)	27.37
		s	25.57	3.08(–2)	30.63
		GP	20.29	5.03(–2)	25.80

In Table I we list the values of the chemical potential (μ), peak gas parameter (x_{pk}), and the half-widths of the column density distributions along with the values of ka considering k-independent s-wave, k-dependent s-wave, and k-dependent $(s+d)$-wave scattering including the LHY term in atom-atom interaction for different values of ka ranging from 1.15 to 3.33. The table also shows the results obtained by solving the GP equation for comparison. For this study the value of ka has been changed by changing the value of a (since the value of k is fixed). Thus the scattering length a has been varied from 3000 a_0 to 8700 a_0 to vary the value of ka from 1.15 to 3.33. By comparing the results (for μ, x_{pk}, and half-width) listed in Table I, it is found that the results for k-independent and k-dependent s-wave interactions differ significantly with the increase in the value of ka. Furthermore, the difference between the results for k-dependent s-wave and $(s+d)$-wave increases with the increase in ka. It is likely that with the increase in ka, the effect of higher partial wave will be prominent in the scattering phenomena. Here we have demonstrated quantitatively that the contribution from the k-dependent d-wave scattering can affect the ground-state properties of BEC significantly for large values of ka. The differences are 59% for μ, 24% for x_{pk}, and 9% for the half-width at $a = 8700 a_0$. Initially the difference in the values of μ, x_{pk}, and half-width for k-dependent s and $(s+d)$-wave interactions is small for $a = 3000\ a_0$, but it increases with the increase in scattering length. Here we attempt to explore the dependence of density profile and the ground-state properties on the value of ka and N of the condensate atoms in the strong interaction region by solving the nonlinear

Schrödinger-like equations considering k-dependent s-wave and higher partial-wave interactions. The values of μ, x_{pk}, and half-width considering k-independent s-wave interaction and the k-dependent s-wave scattering differ significantly even at smaller values of a ($a = 3000\,a_0$), indicating that k-dependent interactions play crucial role in determining the ground-state properties when ka approaches unity and it is greater than unity. We note that for all the results presented here, the LHY correction has been considered both for k-independent and k-dependent interactions. Note that for the k-dependent s-wave scattering μ increases up to $a = 5000\ a_0$ and then decreases. However, this effect is smeared out when the d-wave contribution is added, giving rise to overall increase in μ.

From Table I it is found that the GP results for chemical potential (μ) always lie in between k-independent and k-dependent results, and the value of μ for k-independent interaction (mean field with LHY correction) is the highest compared to others. The GP results for the peak value of the gas parameter at $z = 0$ (x_{pk}) lie very close to those for k-dependent interactions at $a = 3000\ \ a_0$, and it lies in between those for k-dependent s-wave and $(s + d)$-wave interactions with increase of a. However, the value of x_{pk} for k-independent interaction always lies below those for k-dependent interactions and GP results. This shows that the effect of damping due to increase in nonlinearity on the peak density (i.e., peak-gas-parameter) is the strongest for k-independent s-wave interaction, considering the LHY correction for $N = 10\,000$. The k-dependent $(s + d)$-wave results deviate from GP results by 4.8% (for μ), 1.8% (for x_{pk}), and 1.1% (for half-width) at $a = 3000\ a_0$. These deviations increase to 12.3% (for μ), 11.5% (for x_{pk}), and 6% (for half-width) at $a = 8700\ a_0$.

The column densities considering k-dependent s- and $(s + d)$-wave [obtained by solving Eq. (6)] and k-independent s-wave [obtained by solving Eq. (10)] atom-atom scattering are presented in Figs. 1(a), 1(b), and 1(c) for $a = 3000\ a_0$, $7000\ a_0$, and $8700\ a_0$, respectively, for $N = 10\,000$. The dotted and solid lines correspond to the k-dependent s-wave and $(s + d)$-wave scattering; dashed are the k-independent s-wave results; and the circles give the column densities for $(s + d)$-wave scattering considering two-body (K_2) and three-body (K_3) losses [obtained by solving Eq. (9)]. The values of K_2 and K_3 are taken from Fig. 2 in Ref. [20]. For $a = 3000$, 7000, and $8700\ a_0$, the values of K_2 are $5 \times 10^{-19}\ \mathrm{m^3\,s^{-1}}$, $2 \times 10^{-18}\ \mathrm{m^3\,s^{-1}}$, and $4 \times 10^{-18}\ \mathrm{m^3\,s^{-1}}$, respectively, and the values of K_3 are $4.5 \times 10^{-36}\ \mathrm{m^6\,s^{-1}}$, $1 \times 10^{-35}\ \mathrm{m^6\,s^{-1}}$, and $5 \times 10^{-35}\ \mathrm{m^6\,s^{-1}}$, respectively. The triangles in Fig. 1 correspond to the density profiles obtained by solving GP equations. It is found that the column densities for k-dependent s- and $(s + d)$-wave scattering are almost the same for $a = 3000\ a_0$ [Fig. 1(a)]. But with the increase in a, column densities differ significantly for s- and $(s + d)$-wave scattering [Figs. 1(b) and 1(c)]. The contribution from d-wave scattering leads to damping of density at the center of the trap, giving rise to spread of density towards the large values of z. Hence the half-width increases as shown in Table I. At $a = 8700\ a_0$ the deviation in peak density at $z = 0$ for k-dependent s- and $(s + d)$-wave interaction is 20.6%, which can be experimentally detected, where the accuracy of measurement is higher [27]. The contribution from the g-wave interaction to the column density is negligible (less than 1%) for $a = 8700\ a_0$. The column density for k-independent s-wave scattering is further damped at the center of the trap, giving rise to further increase in the half-width for each value of a. Thus for each value of a the column densities for k-dependent and k-independent interactions differ significantly. The GP density near the trap center is lower than the k-dependent density profiles for $a = 3000$ and $7000\ a_0$ but higher than the k-dependent density profile for $a = 8700\ a_0$. A negative contribution arising from the nonlinear interaction term $\frac{3}{4}\frac{g_1^2 - g_2^2}{\epsilon_k^0}|\psi|^4$ in Eq. (6) at $a = 8700\ a_0$ may cause such results.

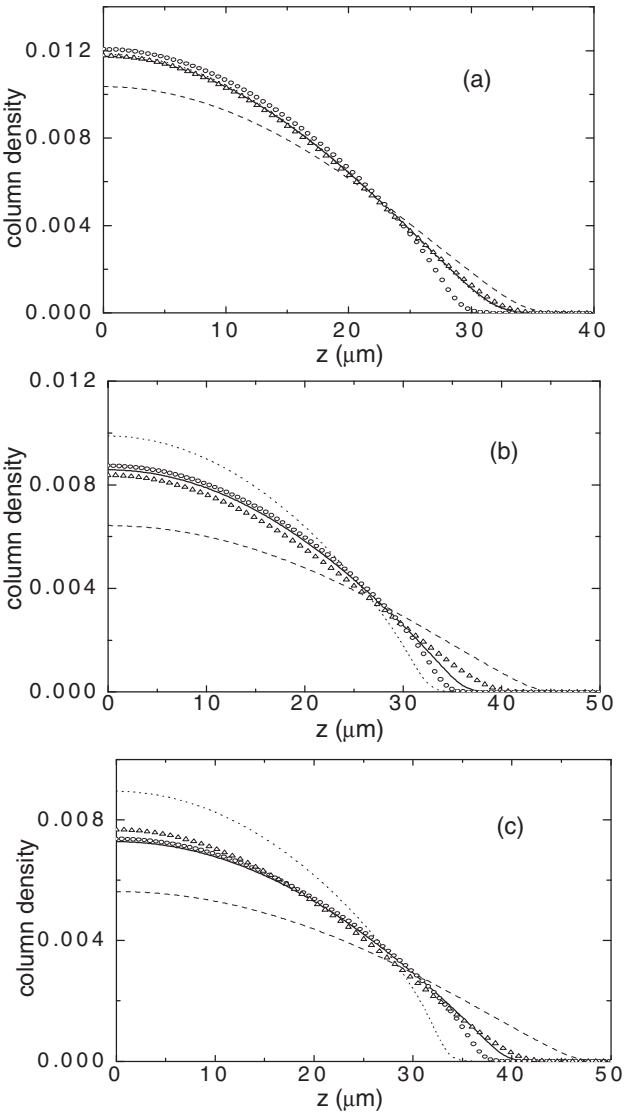

FIG. 1. Column densities of 10^4 ^{85}Rb atoms at (a) $a = 3000\ a_0$, (b) $a = 7000\ a_0$, and (c) $a = 8700\ a_0$ as a function of axial distance (z) for a cylindrical trap with $\omega_\perp/2\pi = 17.5$ Hz and $\omega_z/2\pi = 6.8$ Hz. The vertical axis is multiplied by $2 \times a_\perp^2/N[a_\perp = \sqrt{\hbar/(m\omega_\perp)}]$. The dotted and solid lines represent the densities with k-dependent s-wave and $(s + d)$-wave scattering; dashed lines are the k-independent s-wave results; and the circles give the column density considering two-body (K_2) and three-body (K_3) losses. Triangles represent the GP density profiles.

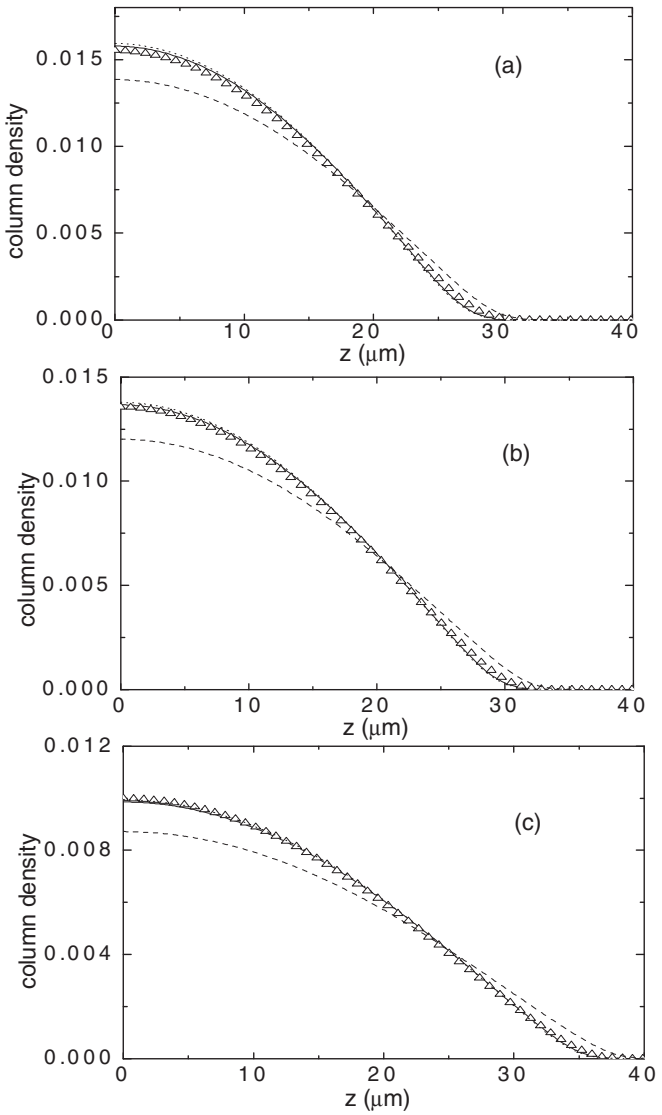

FIG. 2. Column densities of ^{85}Rb atoms at $a = 3000\ a_0$ with $N = 5000$ (a), 7000 (b), and 15 000 (c) as a function of axial distance (z) for a cylindrical trap with $\omega_\perp/2\pi = 17.5$ Hz and $\omega_z/2\pi = 6.8$ Hz. The vertical axis is multiplied by $2 \times a_\perp^2/N[a_\perp = \sqrt{\hbar/(m\omega_\perp)}]$. The dotted and solid lines represent the densities with k-dependent s-wave and $(s + d)$-wave scattering; dashed lines are the k-independent s-wave results. Triangles represent the GP density profiles.

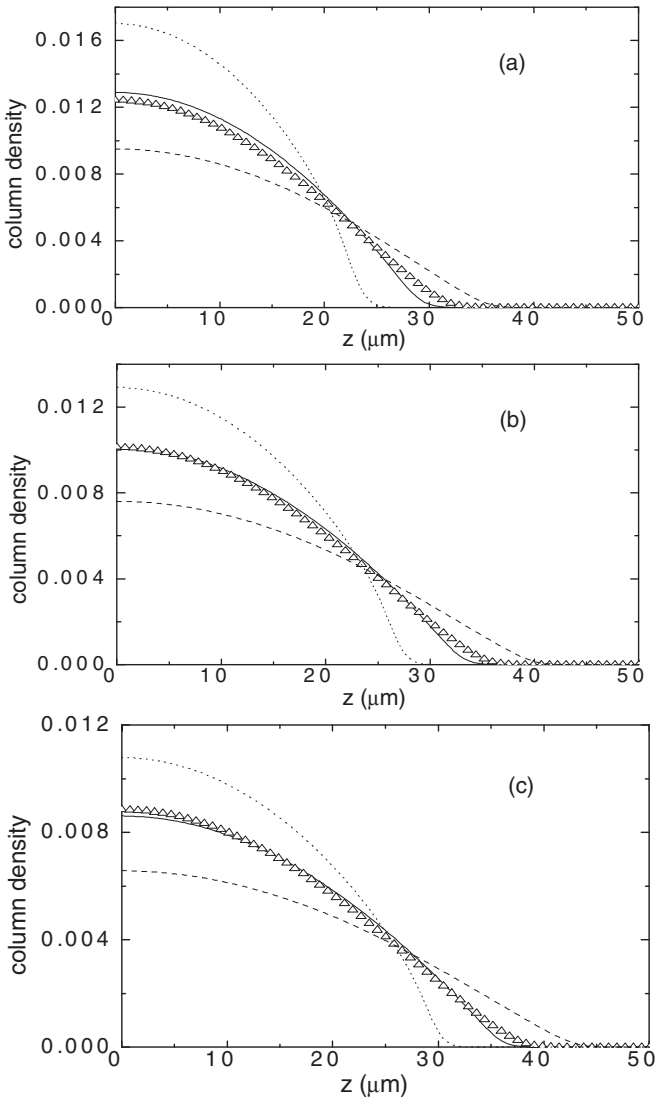

FIG. 3. Column densities of ^{85}Rb atoms at $a = 8700\ a_0$ with $N = 3000$ (a), 5000 (b), and 7000 (c) as a function of axial distance (z) for a cylindrical trap with $\omega_\perp/2\pi = 17.5$ Hz and $\omega_z/2\pi = 6.8$ Hz. The vertical axis is multiplied by $2 \times a_\perp^2/N[a_\perp = \sqrt{\hbar/(m\omega_\perp)}]$. The dotted and solid lines represent the densities with k-dependent s-wave and $(s + d)$-wave scattering; dashed lines are the k-independent s-wave results. Triangles represent the GP density profiles.

It is to be mentioned here that in the present study we have neglected the imaginary part of the k-dependent interaction, which is an approximation. At first order of Beliaev theory it is sufficient to take the real part of the scattering amplitude [3]. Results presented here are valid within this approximation. Nevertheless, one may explore this effect on the density profile in the future.

The column density profiles for the number of atoms $N = 5000$, 7000, and 15 000 are shown in Figs. 2(a), 2(b), and 2(c), respectively, for $a = 3000\ a_0$, and the density profiles with $N = 3000$, 5000, and 7000 are plotted in Figs. 3(a), 3(b), and 3(c), respectively, for $a = 8700\ a_0$. The dotted, solid, and dashed lines correspond to the k-dependent s-wave, k-dependent $(s + d)$-wave, and k-independent s-wave results, respectively. Triangles give the GP column density profile. For a fixed scattering length, as N is increased the nonlinearity keeps on increasing. With the increase in nonlinearity the column densities for both the k-dependent and k-independent interactions are reduced at the center of the trap and expand towards the larger values of z, but the column densities for k-independent and k-dependent interactions differ from each other at each value of N. At each value of N, the peak density for k-independent interaction is always lower than those for k-dependent and GP interactions. The width of density profile for k-independent interaction is larger than the density profiles for other interactions. This feature is also obtained when the scattering length is increased for $N = 10\,000$, as shown in Table I. The increase in nonlinearity

(with increase in N) affects the density profiles for k-dependent and k-independent interactions differently. As a result, the density profiles for k-dependent and k-independent interactions differ with increase in N. Comparison of Figs. 2(a), 2(b), and 2(c) shows that with the increase in N the difference between peak densities at $z = 0$ for k-dependent and k-independent interactions decreases and the difference is 15.4%, 15.1%, and 14.2% for $N = 5000$, 7000, and 15 000, respectively. This is because the damping in the density profile for k-dependent interaction is much faster than that in the density profile for k-independent interaction. At each value of N the GP density profiles are close to those for k-dependent interactions, but it shifts upwards with increase in N. A similar feature has been obtained when a is increased for $N = 10\,000$ (Fig. 1). It is found that at this value of scattering length, $a = 3000\ a_0$, the effect of k-dependent d-wave interaction is negligible and hence the density profiles for k-dependent s-wave and $(s + d)$-wave interactions almost coincide at each value of N (Fig. 2). This shows that the effect of d-wave interactions on the density profile for $a = 3000\ a_0$ is very small even if N is increased.

The effect of strong nonlinearity on density profiles is much more prominent for large values of scattering length $a = 8700\ a_0$ (Fig. 3). First of all, at such large scattering lengths the effect of k-dependent d-wave scattering on the density profile becomes significant even for small values of N, and hence leads to different density profiles for k-dependent s-wave and $(s + d)$-wave interactions at each value of N (3000, 5000, and 7000). The difference between peak density for k-dependent s-wave and $(s + d)$ waves is 24.5%, 21.9%, and 20.4% for $N = 3000$, 5000, and 7000, respectively. Secondly, the effect of damping on the density profiles for k-independent and k-dependent [s-wave and $(s + d)$-wave] interactions differ significantly with increase in N, leading to different density profiles for different types of interactions. The difference between the peak density for k-dependent and k-independent s-wave interactions is 79.7%, 70.1%, and 64.6% for $N = 3000, 5000$, and 7000, respectively. This shows that the difference between the peak density at $z = 0$ for k-independent and k-dependent [s-wave and $(s + d)$-wave] interactions decreases with increase in N, as in the case of $a = 3000\ a_0$. This is due to the fact that the density profiles for different interactions (k-independent, k-dependent, and GP) are affected differently at different values of N. At the value of scattering length $a = 8700\ a_0$, for $N = 3000$, the column density for GP interaction is lower than the column density for $(s + d)$-wave interaction by 3.5%. With the increase in the number of atoms N, the GP and $(s + d)$-wave density profile almost overlap in the central region of the trap. If the value of N is increased to 7000, the GP values of the

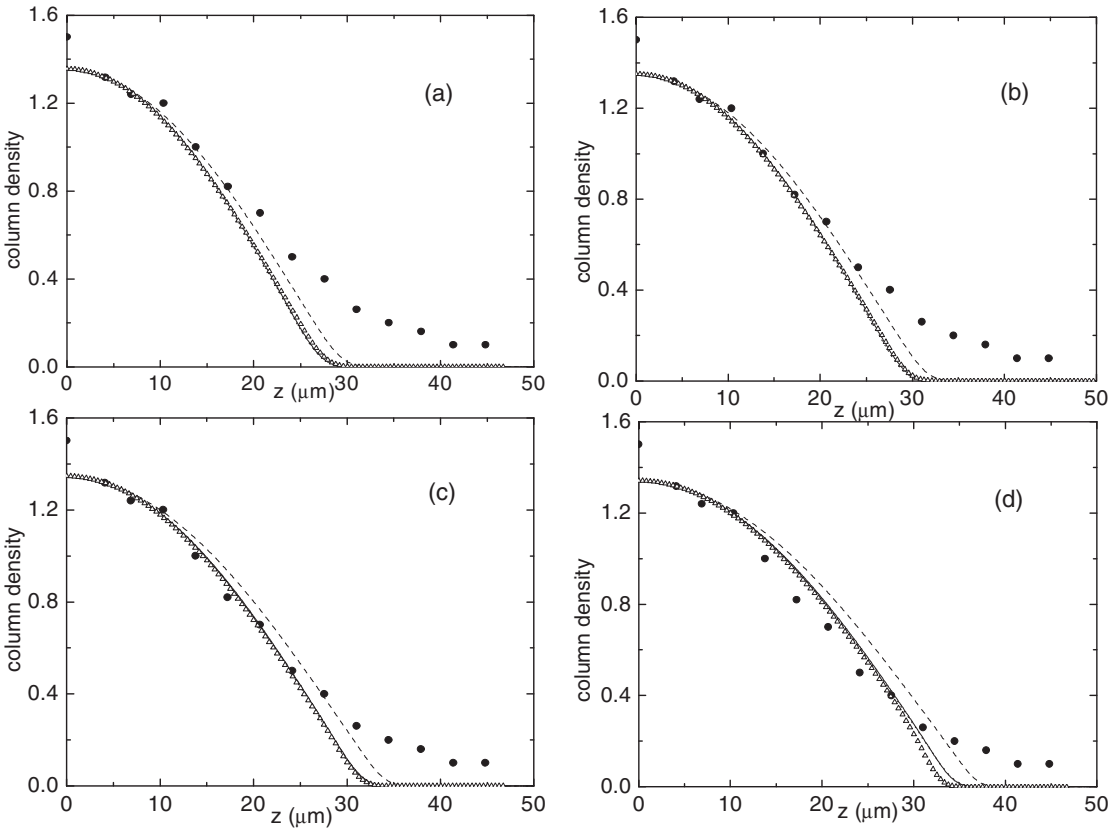

FIG. 4. Column densities of ^{85}Rb atoms for $a = 3000$ and (a) $N = 5000$, (b) $N = 7000$, (c) $N = 10\,000$, and (d) $N = 15\,000$ as a function of axial distance (z) for a cylindrical trap with $\omega_\perp/2\pi = 17.5$ Hz and $\omega_z/2\pi = 6.8$ Hz. The dotted and solid lines represent the densities with k-dependent s-wave and $(s + d)$-wave scattering; dashed lines are the k-independent s-wave results. Triangles represent the GP density profiles. Solid circles are the plots of the experimental condensate column density taken from Fig. 3(d) in Ref. [4].

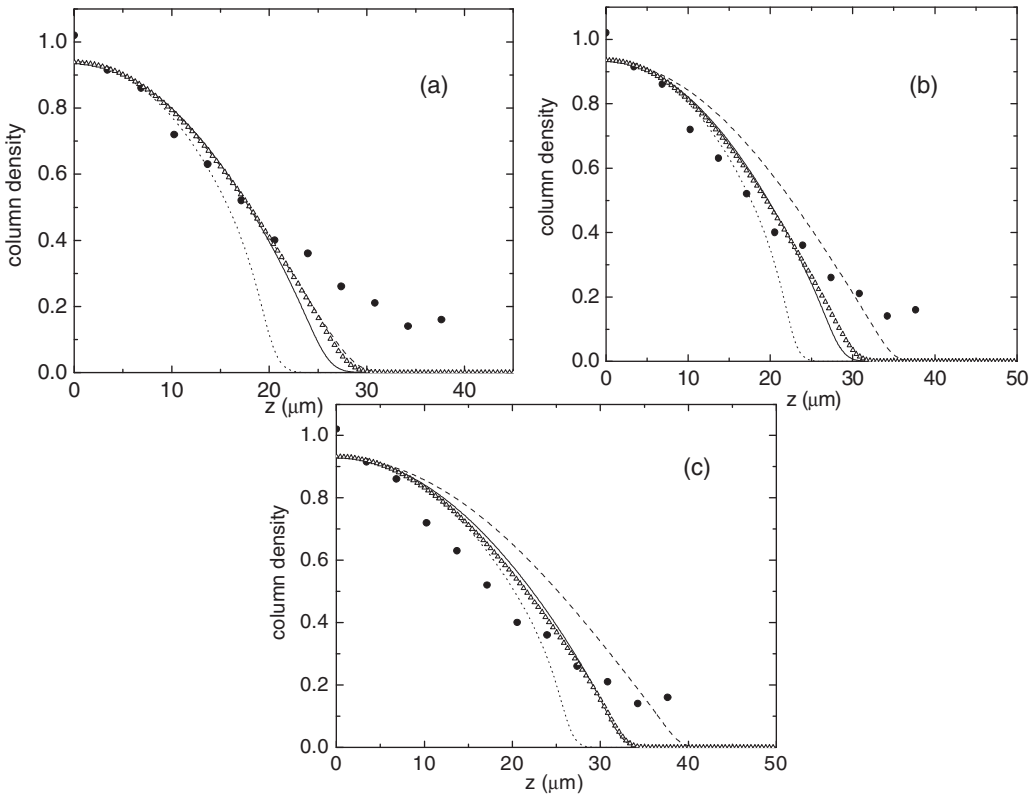

FIG. 5. Column densities of ^{85}Rb atoms for $a = 8700\,a_0$ and (a) $N = 2000$, (b) $N = 3000$, and (c) $N = 5000$ as a function of axial distance (z) for a cylindrical trap with $\omega_\perp/2\pi = 17.5$ Hz and $\omega_z/2\pi = 6.8$ Hz. The dotted and solid lines represent the densities with k-dependent s-wave and $(s+d)$-wave scattering; dashed lines are the k-independent s-wave results. Triangles represent the GP density profiles. Solid circles are the plots of the experimental condensate column density taken from Fig. 3(e) in Ref. [4].

column density become larger than the column density for $(s+d)$-wave interaction by 3.2% [Fig. 3(c)]. A similar feature has been obtained in Fig. 1, where the scattering length has been increased keeping N fixed. This upward shift of the density profiles for GP interaction from those for $(s+d)$-wave interaction with the increase in the interaction strength is due to the negative contribution arising from the difference between the square of the momentum-dependent nonlinear interactions $(g_1^2 - g_2^2)$ in Eq. (6).

In Figs. 4 and 5 the column densities (both due to k-dependent and k-independent interactions) for $a = 3000$ and $8700\,a_0$ considering different values of N have been plotted and compared with the experimental column densities for $B = 157.2$ and 156.4 G, respectively, as given in Figs. 3(d) and 3(e) of Ref. [4]. In the conditions of this experiment the scattering length corresponding to $B = 157.2$ and 156.4 G are 3000 and $8700\,a_0$, respectively (as obtained by manual interpolation from Fig. 1 of Ref. [4]). The dotted and solid lines correspond to the k-dependent s-wave and $(s+d)$-wave scattering; dashed lines are the k-independent s-wave results; triangles give the GP results; and the solid circles are the experimental points. It is well known that column densities of atomic BEC for the ground state obtained by solving the Gross-Pitaevskii or modified Gross-Pitaevskii equations are in general Gaussian and are flat very close to the center of the trap, as shown here. Therefore the sharp fall of the experimental column density around the center of the trap could not be reproduced in this study. Here we have fitted the theoretical column densities with the experimental curve at $z = 4.1$ μm in Fig. 4 and at $z = 3.42$ μm in Fig. 5, respectively. As a result, the theoretical density at $z = 0$ differs from that for experiment by $\sim$10%. In the experiment value of N has been varied from 3000 to 15 000. Since the actual value of N at these two values of magnetic fields is not available [28], for comparison with experiment we have varied N from 2000 to 15 000 at each value of a (3000 and $8700\,a_0$), and we presented here the results for those values of N for which theoretical column densities are comparable to experimental results. In Figs. 4(a)–4(d) we have plotted column densities for $N = 5000$, 7000, 10 000, and 15 000, respectively, for $a = 3000\,a_0$ and those for $a = 8700$ a_0 considering $N = 2000$, 3000, and 5000 have been plotted in Figs. 5(a)–5(c), respectively. Experimental column densities for $a = 3000\,a_0$ (solid circles in Fig. 4) and for $a = 8700\,a_0$ (solid circles in Fig. 5) are obtained by interpolation from Figs. 3(d) (which corresponds to $B = 157.2$ G) and 3(e) (which corresponds to $B = 156.4$ G) in Ref. [4], respectively. As shown before for $a = 3000\,a_0$ (Fig. 2), the fitted theoretical column densities for k-dependent s-wave and $(s+d)$-wave interactions almost coincide, since at this value of scattering length the effect of d-wave interaction is negligible. The density profile for k-independent interaction spreads outward and deviates from those for k-dependent interaction and GP

results for each value of N. By comparing the theoretical density profiles with experimental densities (Fig. 4), it is found that for smaller values of N ($N = 5000$ and 7000) the experimental points are closer to the density profile for k-independent interaction up to $z \sim 25$ μm, but when the value of N is further increased ($N = 10\,000$ and $15\,000$), the experimental points are closer to the density profiles for k-dependent interactions compared to those for k-independent interactions and the agreement is good up to a large value of z (35 μm). Since the result for GP density is close to that for k-dependent interaction in the region of smaller value of z, the experimental density agrees fairly well with GP density in this region, but for larger values of z GP density falls faster than that for k-dependent interaction with an increase in N. This has also been shown in the table (first row) that the half-width for GP is smaller than that for $(s + d)$-wave interaction for $a = 3000\ a_0$ and $N = 10\,000$. Thus the overall agreement of the experimental result with that for k-dependent interaction for large values of N is better than those for other interactions.

For large scattering lengths, $a = 8700\ a_0$, the fitted density profiles for k-dependent s-wave and $(s + d)$-wave interactions differ significantly at different values of N (Fig. 5), similar to that shown in Fig. 3. As mentioned above, since the actual value of N is not known, we have presented the results for N = 2000, 3000, and 5000, which are comparable to the experimental profiles. It is found that for these values of N ($a = 8700\, a_0$), the density profile for mean-field (GP) interaction is close to that for k-dependent $(s + d)$-wave interaction in the region of small value of z and it spreads outward compared to that for k-dependent $(s + d)$-wave interaction with increase in z (for $N = 2000$ and 3000). For these combinations of a and N, the difference between the peak densities for GP and the k-dependent $(s + d)$-wave results varies around 3.5% for change in N from 3000 to 7000. Hence after fitting with experimental value at $z = 3.42$ μm, it appears that both the results [GP and k-dependent $(s + d)$-wave] are in fairly good agreement with experimental values for small values of z, but the difference in the density profiles exists as z is increased (for $N = 2000$ and 3000). The density profile for k-independent interaction (with LHY correction) spreads outwards throughout the range of z considered and the deviation of this density profile from those for k-dependent interactions and GP profiles increases with the increase in N. It is found that for $N = 2000$ experimental densities are closer to the density profiles for k-dependent s-wave interaction for a small value of $z = 20$ μm, after which it spreads outwards. But with the increase in N ($N = 3000$), the agreement between experimental density with those for k-dependent s-wave interaction is good up to $z \sim 30$ μm. With further increase in N ($N = 5000$) the difference between experimental density and k-dependent density profiles increases, since all the density profiles spread outwards due to the increase in nonlinearity. But for all the values of N the density profile for k-independent interaction spreads away from those for k-dependent interactions and hence lie away from the experimental density points. Thus for large scattering length values k-dependent interactions play a crucial role in determining the density profile even at small values of N, leading to fairly good agreement with the experimental results.

However, the long tail away from the center of the trap obtained in the experimental densities could not be explained in this calculation both for $a = 3000\ a_0$ and $8700\ a_0$ (Figs. 4 and 5). To investigate whether this long tail part of the experimental density profile arises due to the evolution of condensate after switching off the trap, we have repeated the calculation to study the time evolution of the condensate after switching off the trap within 0.2 ms. It is found that the column density remains almost the same up to 3 ms, after which it starts to expand, but the column density reported in the experiment was obtained before 3 ms after switching off the trap within 0.2 ms. Therefore the consideration of the evolution of condensate after switching off the trap could not explain the long tail part of the experimental column density. The long tail may occur due to the expansion of heated atoms when the scattering length is increased (i.e., the magnetic field is approaching the value for Feshbach resonance). Therefore this long tail part of the density profile can be explained by considering the interaction due to the high-energy collision of atoms. This long tail part in the experimental density is more prominent for large values of a ($8700\ a_0$), since at this value of scattering length, which is closer to the Feshbach resonance, the atomic cloud becomes very hot, leading to higher atom loss [28]. This explains that for $a = 8700\ a_0$, the agreement between theory and experiment is fairly good for smaller values of N than that for $a = 3000\ a_0$.

IV. SUMMARY

We have shown that the inclusion of the momentum-dependent scattering amplitudes due to s-wave and higher partial waves (d-wave) is important to determine the ground-state properties of the condensate when $ka > 1$ and $x_{pk} \sim 10^{-2}$. Experimentally detectable significant quantitative differences are found between the peak densities for momentum-dependent s- and d-wave interactions. We have shown that theoretical column densities both for $a = 3000$ and $8700\ a_0$ depend on the total number of atoms N. We have also compared the GP column density with that for k-dependent $(s + d)$-wave interaction and found that for small values of N GP density lies below that for k-dependent $(s + d)$-wave interaction, but with increase in N it crosses over to lie above the k-dependent density. The reason for this behavior has been attributed to the effect of a nonlinear term arising from k-dependent interaction. Theoretical column densities for ^{85}Rb atoms considering k-dependent scattering are found to exhibit fairly good agreement with the experimental results for large values of N for small values of scattering length $a = 3000\ a_0$ (corresponding to $B = 157.2$ G) and for small values of N for large values of scattering length $a = 8700\ a_0$ (which correspond to $B = 156.4$ G), respectively.

ACKNOWLEDGMENTS

This work is supported by DST, Government of India, under Project No. SR/S2/LOP-13/2009. We thank Prof. G. V. Shlyapnikov for drawing our attention to the paper of S. T. Beliaev [2].

[1] F. Dalfovo, S. Giorgini, L. Pitaevskii, and S. Stringari, Rev. Mod. Phys. **71**, 463 (1999).
[2] S. T. Beliaev, Zh. Eksp. Teor. Fiz. **34**, 433 (1958) [Sov. Phys. JETP **7**, 299 (1958)].
[3] S. Ronen, J. Phys. B: At. Mol. Opt. Phys. **42**, 055301 (2009).
[4] S. L. Cornish, N. R. Claussen, J. L. Roberts, E. A. Cornell, and C. E. Wieman, Phys. Rev. Lett. **85**, 1795 (2000).
[5] G. Roati, M. Zaccanti, C. DErrico, J. Catani, M. Modugno, A. Simoni, M. Inguscio, and G. Modugno, Phys. Rev. Lett. **99**, 010403 (2007).
[6] S. E. Pollack, D. Dries, M. Junker, Y. P. Chen, T. A. Corcovilos, and R. G. Hulet, Phys. Rev. Lett. **102**, 090402 (2009).
[7] E. A. Donley, N. R. Claussen, S. T. Thompson, and C. E. Wieman, Nature (London) **417**, 529 (2002).
[8] S. T. Thompson, E. Hodby, and C. E. Wieman, Phys. Rev. Lett. **95**, 190404 (2005).
[9] S. Cowell, H. Heiselberg, I. E. Mazets, J. Morales, V. R. Pandharipande, and C. J. Pethick, Phys. Rev. Lett. **88**, 210403 (2002).
[10] E. Braaten, H.-W. Hammer, and T. Mehen, Phys. Rev. Lett. **88**, 040401 (2002).
[11] S. B. Weiss, M. Bhattacharya, and N. P. Bigelow, Phys. Rev. A **68**, 042708 (2003).
[12] S. T. Beliaev, Zh. Eksp. Teor. Fiz. **34**, 417 (1958) [Sov. Phys. JETP **7**, 289 (1958)].
[13] V. I. Klyatskin, Soviet Phys. J. **9**(1), 100 (1966).
[14] P. O. Fedichev and G. V. Shlyapnikov, Phys. Rev. A **58**, 3146 (1998).
[15] N. N. Bogoliubov, J. Phys. (Moscow) **11**, 23 (1947).
[16] T. D. Lee and C. N. Yang, Phys. Rev. **105**, 1119 (1957).
[17] T. D. Lee, K. Huang, and C. N. Yang, Phys. Rev. **106**, 1135 (1957).
[18] K. A. Brueckner and K. Sawada, Phys. Rev. **106**, 1117 (1957).
[19] H. Saito and M. Ueda, Phys. Rev. A **65**, 033624 (2002).
[20] J. L. Roberts, N. R. Claussen, S. L. Cornish, and C. E. Wieman, Phys. Rev. Lett. **85**, 728 (2000).
[21] P. O. Fedichev, M. W. Reynolds, and G. V. Shlyapnikov, Phys. Rev. Lett. **77**, 2921 (1996).
[22] E. Braaten and H.-W. Hammer, Phys. Rev. Lett. **87**, 160407 (2001).
[23] C. J. Pethick and H. Smith, *Bose-Einstein Condensation in Dilute Gases* (Cambridge University Press, Cambridge, UK, 2002).
[24] M. Gupta and K. R. Dastidar, J. Phys. B: At. Mol. Opt. Phys. **41**, 195302 (2008).
[25] M. Gupta and K. R. Dastidar, Phys. Rev. A **81**, 063631 (2010).
[26] A. Fabrocini and A. Polls, Phys. Rev. A **64**, 063610 (2001).
[27] D. M. Stamper-Kurn, H.-J. Miesner, S. Inouye, M. R. Andrews, and W. Ketterle, Phys. Rev. Lett. **81**, 500 (1998).
[28] S. L. Cornish (private communication).